Title

Effects of ferulic acid combined with light irradiation on deoxynivalenol and its production in *Fusarium graminearum*

Author names

Akihiro Shirai [a, b, *], Ami Tanaka [c]

Affiliations

[a] Division of Bioscience and Bioindustry, Graduate School of Technology, Industrial and Social Sciences, Tokushima University, 2-1 Minami-Josanjima, Tokushima 770-8513, Japan.

[b] Institute of Post-LED Photonics, Tokushima University, 2-1 Minami-Josanjima, Tokushima 770-8506, Japan.

[c] Division of Bioresource Science, Graduate School of Sciences and Technology for Innovation, Tokushima University, 2-1 Minami-Josanjima, Tokushima 770-8506, Japan.

*Corresponding author: Akihiro Shirai

Department of Bioscience and Bioindustry, Graduate School of Technology, Industrial and Social Sciences, Tokushima University, 2-1 Minami-Josanjima, Tokushima 770-8506, Japan.

E-mail: a.shirai@tokushima-u.ac.jp

Highlights (85 characters, including spaces, per bullet point; 3 to 5 bullet points)

► Combination of ferulic acid and 365-nm light decreased deoxynivalenol concentration.

► Deoxynivalenol was stable under treatment with light only or ferulic acid only.

► Photoproducts from deoxynivalenol treated with the combination had low toxicity.

► Successive treatment decreased the yields of fungal biomass and deoxynivalenol.

Keywords: Deoxynivalenol, Ferulic acid, Light irradiation, Cytotoxicity, Antifungal assay

ABSTRACT

This study aimed to investigate the effects of ferulic acid (FA), a natural phenolic phytochemical, in combination with light irradiation at three wavelengths (365, 385 and 405 nm) on the concentration and toxicity of deoxynivalenol (DON), a mycotoxin produced by *Fusarium graminearum*. Moreover, this study examined the influence of the combination treatment on DON production in the cultured fungus. FA activated by light at a peak wavelength of 365 nm exhibited the most effective decrease in DON concentration of the tested wavelengths; a residual DON ratio of 0.23 at 24 h exposure was observed, compared with the initial concentration. The reduction in DON using 365-nm light was dependent on the concentration of FA, with a good correlation (r^2=0.979) between the rate constants of DON decrease and FA concentration, which was confirmed by a pseudo-first-order kinetics analysis of the photoreaction with different FA concentrations (50 to 400 mg/L) for 3 h. The viability of HepG2 cells increased by 56.7% following *in vitro* treatment with a mixture containing the photoproducts obtained after treatment with 20 mg/L DON and 200 mg/L FA under 365-nm irradiation for 6 h. These results suggested that the photoreaction of FA under 365-nm irradiation induces the detoxification of DON through degradation or modification of DON. The antifungal effects of the combination (FA and 365-nm light) on *F. graminearum* were investigated. Conidia treated with the combination did not show additive or synergistic

inhibition of fungal biomass and DON production in 7-day cultivated fungal samples compared with samples after single treatment. However, successive treatment, composed of 90 min irradiation at 365 nm and then treatment with 200 mg/L FA for 90 min in the dark, suppressed fungal growth and DON yield to 70% and 25% of the untreated sample level, respectively. This photo-technology involving the two treatment methods of 365-nm irradiation and FA addition as a food-grade phenolic acid in combination or successively, can aid in developing alternative approaches to eliminate fungal contaminants in the fields of environmental water and agriculture. However, further research is required to explore the underlying mechanisms of DON decontamination and its biosynthesis in *F. graminearum*.

1. Introduction

Deoxynivalenol (DON), one of the mycotoxins belonging to type B trichothecenes, is a secondary metabolite produced by *Fusarium* spp. *F. graminearum* is a pathogenic microorganism that is widely distributed in barley and wheat, and causes the disease Fusarium head blight (FHB) (Osborne and Stein, 2007). FHB results in sizeable agricultural losses to farmers (Alshannaq and Yu, 2017) and poses human and animal health risks, such as headache, nutritional disorders, throat irritation, diarrhea, nausea and even death, by ingestion of food and feed containing cereals contaminated with DON (Pestka and Smolinski, 2005). Moreover, the water solubility of DON can potentially cause pollution in environmental water quality (Anater, et al., 2016; Feng et al., 2022), and its stability presents resistance to milling, heating and processing (Sugita-Konishi et al., 2006). It is essential to protect cereals against fungal infection and eliminate mycotoxins to ensure the safety of the water environment, food, and feed.

At present, the available strategies for DON detoxification are divided into three categories: physical, chemical and biological detoxification (Akhila et al., 2021). The physical methods include electromagnetic radiation such as gamma-ray (O'Neill et al., 1993), electron beam (Stepanik et al., 2007), and ultraviolet (UV). A previous study reported that UV radiation decomposed DON in contaminated maize and wheat kernel samples; 253.3-nm irradiation, which is in the UV-C wavelength range, reduced DON content up to 97.3% at the dose of 15 J/cm^2 and *F. graminearum* growth up to 88.8% at the dose of 0.1 J/cm^2 (Popovic et al., 2018). In addition, UV-A radiation, which uses a 368-nm wavelength light source, longer than the UV-C wavelength range, degraded DON content effectively (Jajić et al., 2016). Chemical methods involve the use of chemical reagents such as acids, bases, oxidants, reductants, and chlorinating agents to react with mycotoxins such as aflatoxins. Although such methods are useful for converting mycotoxins to low-toxicity compounds or eliminating them, there are issues with chemical use in terms of practical use, safety, and deterioration of the sensory and functional properties of agricultural products (Méndez-Albores et al., 2007). In contrast, single treatment with citric and lactic acids is milder than the aforementioned methods. Soaking treatment with citric and lactic acids at a 5% concentration for 48 h achieved approx. 50% reduction in the concentration of DON in feed samples spiked with mycotoxins (Humer et al., 2016). Focusing on the application of organic acids to control trichothecene-producing *Fusarium* spp., natural phenolic acids were investigated for their effects on the growth and production of type A trichothecenes using two strains of *Fusarium* spp. Results revealed that mycotoxin production was inhibited in the fungus incubated in the presence of ferulic acid (FA) as one of the phenolic acids assayed, with an accompanying reduction in gene expression involving the mycotoxin biosynthesis pathway, and a reduction in fungal biomass (Ferruz et al., 2016). Other studies

showed that 0.5 mM FA inhibited the accumulation of type B trichothecenes in *Fusarium* sp. by up to 10% compared to the control (Boutigny et al., 2009). However, as far as we know, no studies have been performed in which mycotoxins are decomposed or modified to low toxicity levels through the application of such natural phenolic acids.

Phenolic acids have been evaluated for their photo-bactericidal and -fungicidal activities, and the mechanism of reactive oxygen species (ROS) including superoxide and hydroxyl radicals generation by irradiation in the range from UV-A (365 nm) to violet light (405 nm) (de Oliveira et al., 2021; Nakamura et al., 2015, 2017, 2012; Shirai and Yasutomo, 2019; Shirai et al., 2015, 2022a, 2022b). The photocatalytic reaction of titanium dioxide (TiO_2) is well-known to generate ROS, in contrast to the poorly characterized photoreaction of phenolic acids (Chengbin et al., 2010). The oxidative mechanism has been examined in the decomposition of DON in water and wheat samples and is anticipated to be a promising method, as decomposition approached 91% with 60-min exposure to simulated sunlight (200-2500 nm) (Wu et al., 2020), and there was a reduction in the cytotoxicity of photoproducts (Zhou et al., 2020). Thus, we postulated that the photoreaction of phenolic acids is capable of exhibiting such decomposition activity *via* oxidative action, which is similar to the photocatalytic reaction of TiO_2. At present, few studies have been reported on the elimination and inactivation of DON using light-activated phenolic acids.

We previously demonstrated that among the tested phenolic acids, FA showed the strongest antimicrobial activity with exposure to wavelengths from 365 to 405 nm (Shirai and Yasutomo, 2019; Shirai et al., 2022a). Therefore, FA was used in this study as a food-grade phenolic acid with effective photo-reactivity. The first objective of the study was to investigate the elimination of water-soluble DON using FA activated by light at a wavelength of 365, 385, or 405 nm. Next,

HepG2 cell viability was used to assess the cytotoxicity of the photoproducts after treatment of DON with FA in combination with 365-nm light. The second objective is to determine the effects of the combination of FA and 365-nm irradiation on fungal biomass and DON production yields in *F. graminearum*. Additionally, successive treatment with FA and 365-nm irradiation was evaluated using the antifungal assay. The results of this study could aid in the development of alternative technologies (clean and green technologies) utilizing food-grade phenolic acids and light irradiation in combination for decontamination of mycotoxins in environmental water, food, and feed.

2. Materials and methods

2.1. Chemicals

FA was purchased from the Tokyo Chemical Industry Co., Ltd. (Tokyo, Japan) and dissolved in sterile pure water (Hikari Pharmaceutical Co., Ltd., Tokyo, Japan) at the prescribed concentrations for all experiments. DON (Merck KGaA, Darmstadt, Germany) used as the standard was prepared with sterile pure water at a concentration of 10 or 20 mg/L.

2.2. Light source and irradiation

All assays were performed in an incubator box maintained at 25°C. Irradiation devices equipped with one LED element, 365-, 385- or 405-nm LED (U365, U385 or U405 of NVSU333A series; Nichia Corp., Anan, Japan), were used for all experiments. The peak

140 wavelength and the full width at half maximum for each LED element were 365, 385 or 405 nm
141 and <10 nm according to the data sheet from the manufacturer, respectively. Light exposure of
142 the DON solution and *Fusarium* conidial suspension was performed using glass vials (ϕ15×35
143 mm, 2 mL; Nichiden-Rika Glass Co., Ltd., Kobe, Japan) with lids and plastic Petri dishes (ϕ60
144 mm; AGC Techno Glass Co., Ltd., Shizuoka, Japan) without lids, respectively. For assays of the
145 DON solution treated with light irradiation, the irradiation device was positioned 20 mm from
146 the side of the glass vial containing the DON sample and the irradiance was adjusted to 192
147 mW/cm^2. For the antifungal assay, the Petri dish containing conidia was exposed to 365-nm
148 light from a 50-mm distance above the dish bottom, which generated irradiance of 19 mW/cm^2.
149 During the experimental period of all assays, a small stirring bar (10-mm length) was added into
150 glass vials and Petri dishes containing samples, which were placed on a magnetic stirrer to
151 provide continuous stirring. The irradiance at each distance used was measured using a laser
152 power and energy meter (Nova II; Ophir Optronics Solutions, Ltd., Saitama, Japan) equipped
153 with a photodiode sensor (PD-300-UV; Ophir Optronics Solutions, Ltd.) (Shirai et al., 2017).
154
155 *2.3. Treatment experiment and quantification of DON*
156
157 A mixture of DON (10 mg/L) and FA (200 mg/L) in glass vials was treated with 24-h light
158 exposure at each wavelength, using a 365-, 385-, or 405-nm LED device. Comparative samples
159 without FA or light exposure were prepared under the same condition described above. The
160 DON solution was also mixed with various concentrations of FA (50, 100, 200, and 400 mg/L)
161 prior to exposure to 365-nm light for 6 h.
162 The residual concentration of DON in the mixtures after treatment was analyzed using an

HPLC system equipped with a COSMOSIL column (Cholester, 4.6×150 mm; Nacalai Tesque Inc., Kyoto, Japan) at a flow rate of 0.5 mL/min. The maximum absorbance wavelength of DON (217 nm) was used as the detection wavelength. The mobile phase consisted of methanol containing 0.1% formic acid (solvent A) and 0.1% formic acid aqueous solution (solvent B). The initial composition of solvent A was 20%, then increased to 40% for 30 min, and to 80% for 30 min, and maintained at 80% for 5 min. A peak in the HPLC chromatogram at a retention time of 9.0-10.6 min was assigned as DON. Residual DON concentration was determined using a standard curve of DON over a concentration range of 0.3 to 16 mg/L as shown in Supplemental Fig. A.1 (r^2=0.9988). A retention time from 31.4 to 33.5 min in the same DON chromatogram showed the FA component in the tested solutions, which is shown as the residual ratio from the peak area detected ~~(data not shown)~~.

The reaction of decreasing DON concentration by treatment with FA under 365-nm irradiation was applied to a pseudo-first-order model (Wu et al., 2020), $\ln C = \ln C_0 - kt$, where C_0 represents the initial concentration of DON and C is the residual DON concentration in samples subjected to irradiation at each time point (t). The rate constant k (h^{-1}) of the decrease was calculated from the slope of the linear line at each FA concentration.

2.4. Cell viability assay

Cell viability of HepG2 cells was determined by a colorimetric assay using a cell counting kit-8 (CCK-8; Dojindo Laboratories, Kumamoto, Japan), which estimated the cytotoxicity of photoproducts (including residual DON) after treatment with the combination of FA (200 mg/L) and 365-nm light for 6 h. HepG2 cells were prepared and treated with the photoproducts

according to a previously described method (Zhou et al., 2020). Pre-cultivated cells were incubated with the photoproducts, which were dissolved in Dulbecco's Modified Eagle Medium (DMEM, low glucose; Nacalai Tesque, Inc.) containing 10% fetal bovine serum and 2 mM *L*-glutamine without both phenol red and antibiotics, for 24 h and applied to the CCK-8 for 15 min before measurement of absorbance (*A*) at 450 nm. The viability was compared with that of samples without FA addition or 365-nm light. Cell samples of the negative control, namely 100% dead cells, was prepared by treatment with 1 mol/L hydrogen chloride for 5 min. Control cells (positive) were incubated in the same DMEM as described above. Cell viability (%) was then calculated by $(A_{\text{tested sample}} - A_{\text{dead cells}}) / (A_{\text{positive control cells}} - A_{\text{dead cells}}) \times 100$.

2.5. Fungal strain

F. graminearum Japan Collection of Microorganisms 9873 was purchased from Riken BioResource Research Center (Tsukuba, Japan) and used for experiments.

2.6. Antifungal assay

The conidial suspension of *F. graminearum* was prepared after incubation on potato dextrose agar (PDA; Nissui Pharmaceutical Co. Ltd., Tokyo, Japan) for 14 days at 25°C according to a previously described method (Shirai et al., 2022a). The suspension was adjusted to a density of 1×10^6 conidia/mL with sterile pure water and added as a 100-fold dilution to the plastic Petri dish (final tested volume, 8 mL). The conidial samples to which 200 mg/L FA was added were then irradiated with 365-nm light for 90 min. Assay samples included conidia treated with light

209 only or FA (200 mg/L) only in the dark for an equivalent 90-min duration. A sample was
210 successively treated with 365-nm irradiation followed by 200 mg/L FA (without light) for 90-
211 min respectively. A condition of neither light exposure nor FA addition was used as the control
212 sample. After the treatments, aliquots (0.025 mL) of each suspension were dropped on a 47-mm
213 circular filter membrane with 12-μm pores (polycarbonate, Nuclepore Track-Etch Membrane,
214 Whatman™; GE Healthcare Technologies, Inc., Chicago, IL, USA), which was arranged on a
215 plate (90×15 mm; Sansyo Co., Ltd., Tokyo, Japan) of PDA. The plates were incubated at 25°C
216 for 7 days.
217 The colony formed on the membrane was scrapped up using a spatula and dried *in vacuo*, and
218 then its weight was obtained as the dried fungal biomass yield. Each fungal biomass was placed
219 in a sealed tube, extracted using 5 mL acetonitrile containing 0.1% (v/v) formic acid at 60°C for
220 1 h and centrifuged at 8,600 ×*g* for 10 min, as described previously (Wang et al., 2017a). A 4-
221 mL aliquot of the supernatant was evaporated under nitrogen flow. The residue dissolved in 1
222 mL of acetonitrile:0.1% formic acid (1:1, v/v) was filtered through a 0.22-μm filter (Millex,
223 hydrophilic durapore membrane; Merck KGaA) and analyzed by HPLC to determine the DON
224 concentration, as described in section 2.3. DON content for each fungal biomass was expressed
225 as the weight (mg) per gram of fungal biomass.
226
227 *2.7. Statistical analysis*
228
229 All experiments were performed as three independent experiments, and the results are
230 presented as the mean ± standard deviation. Statistical analyses were performed using either a
231 two-tailed, unpaired Student's *t*-test (Microsoft Excel 365; Microsoft Corporation, Redmond,

232 WA, USA) or a one-way analysis of variance (ANOVA) followed by the Tukey-Kramer
233 honestly significance difference test for multiple comparisons using Excel Tokei ver. 7.0
234 software (Esumi Co., Ltd., Tokyo, Japan). *P* values less than 0.05 were considered significant.
235
236 **3. Results**
237
238 *3.1. Effects of combinations of FA and light irradiation on DON content*
239
240 The effects of combinations of FA and light at different wavelengths (365, 385, or 405 nm)
241 were assessed using a DON solution at an initial concentration of 10 mg/L (C_0). Figure 1 (A)
242 shows the time-course changes in DON residual ratios (C/C_0) under irradiation at each
243 wavelength as a function of time: C is the residual concentration of DON irradiated at different
244 times. The combination of 200 mg/L FA and 365-nm light decreased the DON residual ratio to
245 0.73 ± 0.04 at 3-h illumination. Furthermore, the illumination for 6 and 24 h significantly
246 decreased DON ratios to 0.62 ± 0.03 and 0.23 ± 0.04, respectively. When the DON solution was
247 irradiated at 385 nm or 405 nm with FA, similar time-dependent trends in decreasing DON
248 residual ratios were observed as for the 365-nm light described above. However, the residual
249 DON ratios after 24-h irradiation were much higher than that with 365-nm light; DON ratios of
250 0.58 ± 0.08 under 385-nm irradiation and 0.79 ± 0.07 under 405-nm irradiation were observed.
251 Residual FA contents were detected simultaneously when DON contents were measured during
252 the experimental period. FA content at each wavelength tested decreased gradually as the
253 irradiation time was extended to 24 h, as shown in Supplemental Fig. B.1. The combination
254 with 365-nm light gave the fastest reduction in FA content among the three wavelengths tested.

When the DON solution was exposed to 365-nm light without FA, there was a significant decrease in DON ratio up to 0.84 ± 0.01 at 24-h irradiation, but not to the level of the combination with FA (Fig. 1 (B)). Irradiation treatments with other wavelengths, 385 and 405 nm, and FA only treatment scarcely affected DON content, even at a treatment time of 24 h.

The effect on water-soluble DON under irradiation was investigated at FA concentrations of 50, 100, 200, or 400 mg/L in combination with 365-nm light exposure for 6 h. As FA concentration was increased in the DON solution, the concentrations of residual DON following irradiation declined; the time-course change in DON ratio increased with the increase in FA concentration (Fig. 2 (A)). In addition to the results of the reduction in DON ratio, an irradiation time-dependent reduction in FA content was also confirmed (Supplemental Fig. C.1). As the reduction in the ln-DON ratio after each combined treatment at different FA concentrations showed a linear trend versus irradiation time up to 3 h in Supplemental Fig. C.2, the reaction of decreasing DON concentration was applied to a pseudo-first-order model (Wu et al., 2020). The rate constant k (h^{-1}) of the decrease was calculated from the slope of the linear line at each FA concentration. The k values were 0.037 ± 0.011, 0.077 ± 0.025, 0.106 ± 0.032, and 0.214 ± 0.024 for 50, 100, 200, and 400 mg/L FA, respectively. In Fig. 2 (B), values of the logarithms of k were confirmed to correlate to those of the initial concentrations of FA. The regression analysis indicated an r^2 of 0.979 and the FA concentration was a significant variable (P <0.01). Photo-treatment of DON with FA at 400 mg/L over 3 h attenuated the decrease rate constant to 0.061 ± 0.019. This value did not differ from the rate constant at 100 mg/L FA during the initial 3 h of irradiation (P > 0.05; t-test).

3.2. Effect of DON photoproducts following combined treatment on cell viability

278

279 To evaluate the cytotoxicity of the DON photoproducts after treatment with the combination of
280 FA (200 mg/L) and 365-nm light for 6 h, the viability of HepG2 cells was assayed using a CCK-
281 8 assay. DON samples (untreated) maintained for 6 h in the absence of both FA and light
282 exhibited 27.9 ± 3.7% viability, which was a negligible increase in viability compared with the
283 initial samples (25.8 ± 2.5% viability) in Fig. 3. The sample treated with FA in the dark for 6 h
284 also showed no significant change in cell viability compared with the sample before treatment.
285 A small increase in viability was observed in samples before and after exposure to 365-nm light,
286 from 26.2 ± 0.9 to 34.2 ± 6.1%, but the change was not significant ($P > 0.05$; *t*-test). On the
287 other hand, cells exposed to the photoproducts following combination treatment with FA and
288 light exhibited 56.7 ± 4.9% viability, which was much higher than the initial sample (32.9 ±
289 3.7% viability). From the HPLC analysis of the photoproduct samples, the DON concentration
290 in the mixture was decreased from 20.0 ± 0.8 to 10.9 ± 0.7 mg/L (45% reduction in DON
291 concentration).

292

293 *3.3. Effects of combination and successive treatments on DON production in F. graminearum*

294

295 Yields of dry fungal biomass and DON were investigated in 7-day cultivated fungi after 90-
296 min treatment with each condition: 365-nm light alone, 200 mg/L FA alone, the combination of
297 those conditions, and successive treatment with light irradiation and FA (90-min light exposure
298 followed by 90-min treatment with FA in the dark). The yields were compared to those for
299 untreated samples (control) without both light and FA. Subsequent to treatment with light
300 irradiation or FA alone and their combination, the cultured fungi including control samples

produced almost the same amount of biomass, which ranged from 9.4 to 11.5 mg (Fig. 4 (A)). Only the successive treatment significantly decreased the fungal biomass to 8.0 mg, which was comparable to 70% of the control biomass level. Next, the DON content extracted from the fungal biomass was determined. Figure 4 (B) shows that treatments with light irradiation alone, FA alone, and the combination decreased the DON yields to 0.188 ± 0.020, 0.139 ± 0.011 and 0.161 ± 0.025 mg per gram of fungal biomass, respectively, corresponding to yield levels ranging from 53 to 71% of the control samples (0.264 ± 0.022 mg/g of fungal biomass). However, no differences in DON yield were observed among the three treatment conditions. The DON yield for fungi treated successively with light irradiation and FA differed markedly from the other conditions, showing 0.067 ± 0.016 mg yield, which was 25% of the control yield.

4. Discussion

The application of FA with 365- and 405-nm light showed improved antimicrobial activity, which was attributed to synergistic efficiency generated by ROS production (hydrogen peroxide and hydroxyl radicals) through FA activation by light irradiation, confirmed quantitatively or qualitatively by a colorimetric method and an electron spin resonance method (Shirai et al., 2022a, 2022b). Although DON is stable, e.g., shows heat resistance (Sugita-Konishi et al., 2006), nanoparticles coated with TiO_2 decomposed DON *via* photocatalytic action under simulated sunlight irradiation (Wu et al., 2020; Zhou et al., 2020). In reference to these previous assays, an initial DON concentration of 10 or 20 mg/L was chosen for our experiments.

For phenolic acids, a shorter wavelength showed stronger bactericidal activity, which was attributed to the production of greater amounts of ROS (Nakamura et al., 2017). ROS

production through the FA photoreaction was presumed to affect the reduction in DON ratio for each wavelength used; the results revealed that the combination with a shorter wavelength (365 nm) of irradiation produced the greatest decrease in DON in this work. Simultaneously, the rapid reduction in FA content in the reactant indicated that the high photo-reactivity is dependent on the wavelength. Furthermore, the small time-course change in DON ratio following single treatment with irradiation demonstrated the value of using FA in combination with 365-nm irradiation. In our results, since residual DON ratios were decreased greatly during 6-h irradiation at 365 nm in the presence of FA, the effect of FA concentration on DON elimination was investigated to elucidate in detail whether the FA photoreaction involves decreases in DON concentration. The correlation between the logarithms of the rate constants of DON decrease and FA concentrations showed that the rate constant became increasingly large with increases in FA concentration. The correlation could explain DON elimination by FA photoreaction, which generates ROS *via* photo-oxidation of the molecule. We consider that the gradual reduction in FA content during irradiation resulted in attenuation of the rate constant of DON decrease when irradiation continued for more than 3 h. Photo-oxidation of FA might have caused a transformation of the photo-reactivity to lower than the original FA, attributed to dimerization and radical-radial coupling related to the radical molecules derived from FA (Amic et al., 2020). This suggests that the activated FA could modify the structure of DON, leading to a reduction in the original DON content.

Although the combination of FA and 365-nm light decreased the original DON content effectively, it is important to evaluate whether the toxicity of the photoproducts following treatment was reduced compared to before treatment. Photoproducts after 6-h irradiation in the presence of FA were confirmed to exhibit lower cytotoxicity than the samples before irradiation.

Measurement of cell viability determined the IC_{50} of DON to be 9.1 mg/L (data not shown), implying that the cell viability of the photoproducts reflected the cytotoxicity of the original DON (10.9 mg/L) remaining in the photo-reactant. In contrast to the decline in toxicity, the stability of DON was demonstrated by the results of no change in cytotoxicity of DON samples following single treatment with 365-nm light or FA. In a previous report, exposure of maize samples contaminated with DON to a 368-nm UV lamp decomposed DON up to 16% of the control level (Jajić et al., 2016). Differences in the reduction efficiency could be attributed to the UV power used in experiments. The result that FA (in the dark) showed unchanged DON cytotoxicity corresponded to a report that citric acid did not change the concentration of DON spiked to feed samples following soaking in a 5% solution for 24 h (Humer et al., 2016), as well as our result of DON quantification in the presence of FA without light. It was concluded that the synergistic action of the combination of FA and light can effectively detoxify DON.

The C12-C13-epoxy group and the hydroxyl substituent at the 3-position of the DON structure are reported to be essential for toxicity; destruction of the group and modification with glycoside or acetylation of the substituent abrogate the toxicity (Eriksen et al., 2004; Pierron et al., 2016; Young et al., 2006). Therefore, in this study, it was inferred that structural changes in DON contribute to a reduction in cytotoxicity following combination treatment. Breaks in the double bond and epoxy group of the DON structure were estimated by photo-treatment with TiO_2 (Wu et al., 2020; Zhou et al., 2020). We will continue to study the detoxification mechanism in future work. The DON degradation method using TiO_2 photocatalysis was more effective than our combination; however, it is necessary to remove the nanoparticles using a separation process, such as centrifugation or filtration, from the reactant (Zhou et al., 2020). On the other hand, our combination does not require a separation process, since the photoproducts

following combination treatment possess lower toxicity than the initial DON samples including FA.

It is an important subject to control the physiological activity of *Fusarium* spp., i.e., growth and mycotoxin production, to prevent harm from FHB. To investigate the effect of FA with 365-nm irradiation on DON-biosynthesizing *F. graminearum*, the fungal biomass and DON yields after treatment were analyzed. Conidia treated with each condition were cultivated for 7 days on a membrane filter placed on top of the PDA surface. This method avoided contamination with components from the broth culture to the collected fungal and extracted samples before HPLC analysis, unlike previously described methods in which the mycotoxin was extracted from the broth supernatant (Boutigny et al., 2009) or agar block (Fanelli et al., 2012) cultivated with the tested fungi.

It is reported that FA inhibits not only the mycelial growth of *Fusarium* spp. but also the production of mycotoxins such as DON (Boutigny et al., 2009), zearalenone (Schöneberg et al., 2018), and fumonisin (Ferrochio et al., 2013). Meanwhile, in some strains of *Fusarium* spp., cultivation in the presence of FA (from 0.5 to 10 mM) accelerated growth or mycotoxin production compared to the condition without FA (Ferrochio et al., 2013; Ferruz et al., 2016). There are conflicting reports on the effects of FA on physiological activity. In this study using a strain of *F. graminearum*, FA treatment decreased DON yields but did not significantly change the fungal biomass weight as compared with the control. Continuous 390-nm irradiation during 10-day cultivation, which is similar to the wavelength used in this study, inhibited both growth and fumonisin production in a *Fusarium* sp. (Fanelli et al., 2012). According to the results obtained in this study, the effect of exposure of conidial samples to 365-nm light for 90 min on growth and DON production was identical with that of FA treatment. Our findings in the strain

of *F. graminearum* suggest that the sublethal doses of FA and light exposure show separate physiological effects that inhibit DON production, despite the essentially unchanged fungal growth. This relationship implies some malfunction in biosynthesis ability aside from fungal growth. As described in some reports, the repression of DON production could be related to reduced expression levels of *Tri* gene transcripts related to DON biosynthesis in *Fusarium* spp. exposed to FA and illumination singly (Boutigny et al., 2009; Fanelli et al., 2012; Ferruz et al., 2016). From the presumed mechanisms of DON repression, it seems that the inhibitory mechanisms of fungal growth by phenolic acids and light exposure are independent of the inhibitory mechanisms involved in mycotoxin production (Ferruz et al., 2016; Suzuki, 2018). This suggestion is supported by the results obtained by Suzuki (2018), in which an *Aspergillus* strain subjected to 401-nm violet irradiation showed increased aflatoxin production but low growth.

Determination of the yields of fungal biomass and DON in *F. graminearum* cultivated after treatment with FA and 365-nm light in combination showed almost the same relationship as single treatment; namely, the combination did not show additive or synergistic effects. ROS generated excessively *via* light-activated FA act as strong molecules in the combination treatment and differ from individual treatment. However, the oxidative action against conidia might not have increased due to interference from the rigid cell wall structure in terms of permeating the cell wall and then acting within the cell to effectively damage cell functions. The change from a synchronized combination (as described above) to a successive process of 365-nm irradiation followed by FA treatment produced an additive effect, i.e., the effect of irradiation was added to that of FA addition, which strongly suppressed DON yields and reduced fungal biomass. This result is interesting in that the ability for both growth and DON

production deteriorated more than for the other treatments tested including the synchronized treatment. Oxidative damage by exposure to UV-A light is known to induce membrane dysfunction and increase the membrane permeability of bacteria (Bosshard et al., 2010). UV-A irradiation induced bacterial cells to incorporate more gallic acid into the cells (Wang et al., 2017b). Therefore, in addition to inhibition of cell functions, UV-A irradiation prior to FA treatment contributed oxidative damage to conidial cell walls, thereby increasing the uptake of FA to conidia. The fungal metabolism for both growth and DON biosynthesis might have been altered by the additive oxidative action of the incorporated FA into conidia since phenolic acids such as FA have a prooxidant effect to induce ROS generation (Gomes, 2003). For instance, the single treatment with FA decreased ATP content in yeast cells (Shirai et al., 2022b). It was suggested that the intracellular localization of FA plays an important role in its action on fungal metabolism in conjunction with the oxidative effects of ROS, even if ROS generation was promoted when FA was exposed to 365-nm light. Indeed, oxidative damage to cytosolic proteins rather than loss of membrane integrity was observed using FA and UV-A in combination for inactivation of yeast cells (Shirai et al., 2022b). Further studies are required to elucidate the mechanism of the successive treatment effects, focusing on the increased incorporation of FA molecules and subsequent ROS generation within conidia, as well as from the perspective of the expression level of *Tri* gene transcripts in the DON biosynthetic pathway.

5. Conclusion

The time-course change in DON concentration in response to three light wavelengths (365, 385, and 405 nm) combined with FA varied depending on the wavelength used; the combination

with 365-nm light decreased the DON concentration effectively. The reduction in DON concentration by photo-treatment with 365-nm light was investigated by varying the FA concentration employed (50, 100, 200, and 400 mg/L). We applied a pseudo-first-order model to analyze the reaction with photo-treatment on DON and concluded that the rate constant of DON decrease is correlated to the FA concentration, suggesting that FA photoreaction, which generates excessive ROS, contributed to the reduction in DON. Cytotoxicity data revealed detoxification of DON after treatment with the combination of FA and 365-nm light, indicating its chemical degradation or modification during the FA photoreaction. The most effective combination to reduce the concentration and cytotoxicity of DON did not show additive or synergistic inhibition against fungal biomass and DON yields in a strain of *F. graminearum* cultivated. However, a novel successive process, in which the conidia were subjected to 365-nm light followed by FA treatment, was observed to suppress DON production and fungal growth. The results of this study present the alternative application of FA and 365-nm light as a potential approach for the protection of environmental water quality and decontamination of food and feed.

Author contributions

A. Shirai designed the study and the two authors including A. Tanaka collected the data; A. Shirai wrote and edited the manuscript. All authors have approved the manuscript.

Declaration of competing interest

The authors declare that there are no conflicts of interest regarding the publication of this paper.

Acknowledgments

This work was supported by a Grant-in-Aid for Scientific Research (B) from the Japan Society for the Promotion of Science (~~No.~~ JP23H02348). The authors thank FORTE Science Communications (https://www.forte-science.co.jp/) for English language editing.

Appendix A. Supplementary data

Supplementary data for this article, Figs. A.1, B.1, C.1 and C.2, can be found online.

Fig. A.1. A regression line generated from plots of the detected area assigned as DON by HPLC analysis against known concentrations of DON: detected area assigned as DON = -1446.3 + 71277 × (DON conc.) (r^2 = 0.9988). Plot data are presented as means ± SD (n=3).

Fig. B.1. Time-course change in residual FA ratios (C/C_0) in samples exposed to different light wavelengths (365 (○), 385 (△), and 405 (□) nm) for each irradiation time. FA contents were measured at the same time as DON analysis by HPLC, corresponding to Fig. 1 (A). C_0 and C represent the area of FA detected with HPLC analysis before and after light irradiation, respectively. Plot data are presented as means ± SD (n=3).

Fig. C.1. Time-course change in residual FA ratios (C/C_0) in samples exposed to different FA concentrations (50 (×), 100 (△), 200 (○), and 400 (□) mg/L) for each irradiation time. FA

485 contents were measured at the same time as DON analysis by HPLC, corresponding to Fig. 2
486 (A). C_0 and C represent the area of FA detected with HPLC analysis before and after light
487 irradiation, respectively. Data are presented as means ± SD (n=3).
488
489 **Fig. C.2.** Pseudo-first order kinetics corresponding to Fig. 2 (A). Symbols represent 50 (×), 100
490 (△), 200 (○), and 400 (□) mg/L FA. Data are presented as means ± SD (n=3).
491
492 **Figure captions**
493
494 **Fig. 1.** Changes in DON contents under different light wavelengths (365 (○), 385 (△), and 405
495 (□) nm), in the photo-treatment of 10 mg/L DON. Panels A and B show the ratios of DON
496 concentration (C/C_0) after treatments with each light exposure combined with 200 mg/L FA
497 (panel A) and with irradiation alone in addition to FA alone (+) (panel B), respectively. C_0
498 represents the initial concentration of DON and C is the residual DON concentration in samples
499 subjected to irradiation or incubation at each time point. Data are presented as means ± SD
500 (n=3).
501
502 **Fig. 2.** Changes in DON contents under different FA concentrations (50 (×), 100 (△), 200 (○),
503 and 400 (□) mg/L), with 365-nm irradiation in the photo-treatment of 10 mg/L DON. Panels A
504 and B show the ratios of DON concentration (C/C_0) after the photo-treatments combined with
505 each FA concentration (panel A) and a regression line between the logarithms of the rate
506 constant of DON decrease, k (h^{-1}), and of the tested FA concentration, C_{FA} (mg/L) (panel B),
507 respectively: $\log k = -2.8097 + 0.81418 \times (\log C_{FA})$ ($r^2 = 0.9789$). Data are presented as means ±

508 SD (n=3).

509

510 **Fig. 3.** Effect of DON samples before and after each treatment on HepG2 cell viability. DON
511 (20 mg/L) was treated with 365-nm irradiation alone, 200-mg/L FA alone, and their combination
512 for 6 h each; shaded bars, initial samples before each treatment; open bars, samples after each 6-
513 h treatment. Control samples were neither light exposure nor FA addition. Data are presented as
514 means ± SD. Significant differences (**$P < 0.01$; two-tailed, unpaired *t*-test) were calculated
515 based on comparisons of viability between the initial and 6-h treatment. n.s., not significant.

516

517 **Fig. 4.** Effects of each treatment on fungal biomass (A) and DON yield (B). *F. graminearum*
518 conidia were treated with each condition for 90 min as follows: 1, control (without both light
519 and FA); 2, 365-nm light alone; 3, 200-mg/L FA alone; 4, the combination of light and FA; 5,
520 successive process (exposure to 365-nm light for 90 min followed by FA treatment for 90 min in
521 the dark). Data are presented as means ± SD (n=3). Different letters above the columns refer to
522 significant differences between groups ($P < 0.01$ and only $P < 0.05$ between samples 2 and 5 in
523 panel A, $P < 0.01$ in panel B; one-way ANOVA).

524

525 **References**

526

527 Akhila, P.P., Sunooj, K.V., Aaliya, B., Navaf, M., Sudheesh, C., Sabu, S., Sasidharan, A., Mir,
528 S.A., George, J., Mousavi Khaneghah, A., 2021. Application of electromagnetic radiations
529 for decontamination of fungi and mycotoxins in food products: A comprehensive review.
530 Trends Food Sci. Technol. **114**, 399-409.

Alshannaq, A., Yu, J.H., 2017. Occurrence, toxicity, and analysis of major mycotoxins in food. Int. J. Env. Res. Public Health **14**, 632.

Amic, A., Markovic, Z., Dimitric Markovic, J.M., Milenkovic, D., Stepanic, V., 2020. Antioxidative potential of ferulic acid phenoxyl radical. Phytochemistry **170**, 112218.

Anater, A., Manyes, L., Meca, G., Ferrer, E., Luciano, F.B., Pimpão, C.T., Font, G., 2016. Mycotoxins and their consequences in aquaculture: A review. Aquaculture **451**, 1-10.

Bosshard, F., Bucheli, M., Meur, Y., Egli, T., 2010. The respiratory chain is the cell's Achilles' heel during UVA inactivation in *Escherichia coli*. Microbiology **156**, 2006-2015.

Boutigny, A.L., Barreau, C., Atanasova-Penichon, V., Verdal-Bonnin, M.N., Pinson-Gadais, L., Richard-Forget, F., 2009. Ferulic acid, an efficient inhibitor of type B trichothecene biosynthesis and *Tri* gene expression in *Fusarium* liquid cultures. Mycol. Res. **113**, 746-753.

Chengbin, X., Jianhong, W., Fengli, L., Wei, L., Xiangliang, Y., Fandian, Z., Huibi, X., 2010. Nano titanium dioxide induces the generation of ROS and potential damage in HaCaT cells under UVA irradiation. J. Nanosci. Nanotechnol. **10**, 8500-8507.

de Oliveira, E.F., Yang, X., Basnayake, N., Huu, C.N., Wang, L., Tikekar, R., Nitin, N., 2021. Screening of antimicrobial synergism between phenolic acids derivatives and UV-A light radiation. J. Photochem. Photobiol. B: Biol. **214**, 112081.

Eriksen, G.S., Pettersson, H., Lundh, T., 2004. Comparative cytotoxicity of deoxynivalenol, nivalenol, their acetylated derivatives and de-epoxy metabolites. Food Chem. Toxicol. **42**, 619-624.

Fanelli, F., Schmidt-Heydt, M., Haidukowski, M., Susca, A., Geisen, R., Logrieco, A., Mule, G., 2012. Influence of light on growth, conidiation and fumonisin production by *Fusarium verticillioides*. Fungal Biol. **116**, 241-248.

554 Ferrochio, L., Cendoya, E., Farnochi, M.C., Massad, W., Ramirez, M.L., 2013. Evaluation of
555 ability of ferulic acid to control growth and fumonisin production of *Fusarium*
556 *verticillioides* and *Fusarium proliferatum* on maize based media. Int. J. Food Microbiol. **167**,
557 215-220.
558 Feng, J., Xue, Y., Wang, X., Song, Q., Wang, B., Ren, X., Zhang, L., Liu, Z., 2022. Sensitive,
559 simultaneous and quantitative detection of deoxynivalenol and fumonisin B1 in the water
560 environment using lateral flow immunoassay integrated with smartphone. Sci. Total Environ.
561 **834**, 155354.
562 Ferruz, E., Atanasova-Penichon, V., Bonnin-Verdal, M.N., Marchegay, G., Pinson-Gadais, L.,
563 Ducos, C., Loran, S., Arino, A., Barreau, C., Richard-Forget, F., 2016. Effects of phenolic
564 acids on the growth and production of T-2 and HT-2 toxins by *Fusarium langsethiae* and *F.*
565 *sporotrichioides*. Molecules **21**, 449.
566 Gomes, C.A.d.C., T. G.; Andrade, J. L.; Milhazes, N.; Borges, F.; Marques, M. P., 2003.
567 Anticancer activity of phenolic acids of natural or synthetic origin: A structure-activity study.
568 J. Med. Chem. **46**, 5395-5401.
569 Humer, E., Lucke, A., Harder, H., Metzler-Zebeli, B.U., Bohm, J., Zebeli, Q., 2016. Effects of
570 citric and lactic acid on the reduction of deoxynivalenol and its derivatives in feeds. Toxins
571 **8**, 285.
572 Jajić, I., Jakšić, S., Krstović, S., Abramović, B., 2016. Preliminary results on deoxynivalenol
573 degradation in maize by UVA and UVC irradiation. Contemporary Agriculture **65**, 7-12.
574 Méndez-Albores, A., Del Río-García, J.C., Moreno-Martínez, E., 2007. Decontamination of
575 aflatoxin duckling feed with aqueous citric acid treatment. Anim. Feed Sci. Technol. **135**,
576 249-262.

577 Nakamura, K., Ishiyama, K., Sheng, H., Ikai, H., Kanno, T., Niwano, Y., 2015. Bactericidal
578 activity and mechanism of photoirradiated polyphenols against gram-positive and -negative
579 bacteria. J. Agric. Food Chem. **63**, 7707-7713.
580 Nakamura, K., Shirato, M., Kanno, T., Lingstrom, P., Ortengren, U., Niwano, Y., 2017. Photo-
581 irradiated caffeic acid exhibits antimicrobial activity against *Streptococcus mutans* biofilms
582 via hydroxyl radical formation. Scientific Reports **7**, 6353.
583 O'Neill, K., Damoglou, A.P., Patterson, M.F., 1993. The stability of deoxynivalenol and 3-acetyl
584 deoxynivalenol to gamma irradiation. Food Addit. Contam. **10**, 209-215.
585 Osborne, L.E., Stein, J.M., 2007. Epidemiology of Fusarium head blight on small-grain cereals.
586 Int. J. Food Microbiol. **119**, 103-108.
587 Pestka, J.J., Smolinski, A.T., 2005. Deoxynivalenol: toxicology and potential effects on humans.
588 J. Toxicol. Environ. Health, Part B **8**, 39-69.
589 Pierron, A., Mimoun, S., Murate, L.S., Loiseau, N., Lippi, Y., Bracarense, A.P., Liaubet, L.,
590 Schatzmayr, G., Berthiller, F., Moll, W.D., Oswald, I.P., 2016. Intestinal toxicity of the
591 masked mycotoxin deoxynivalenol-3-β-D-glucoside. Arch. Toxicol. **90**, 2037-2046.
592 Popovic, V., Fairbanks, N., Pierscianowski, J., Biancaniello, M., Zhou, T., Koutchma, T., 2018.
593 Feasibility of 3D UV-C treatment to reduce fungal growth and mycotoxin loads on maize
594 and wheat kernels. Mycotoxin Rese. **34**, 211-221.
595 Schöneberg, T., Kibler, K., Sulyok, M., Musa, T., Bucheli, T.D., Mascher, F., Bertossa, M.,
596 Voegele, R.T., Vogelgsang, S., 2018. Can plant phenolic compounds reduce *Fusarium*
597 growth and mycotoxin production in cereals? Food Addit. Contam. Part A **35**, 2455-2470.
598 Shirai, A., Kajiura, M., Omasa, T., 2015. Synergistic photobactericidal activity based on
599 ultraviolet-A irradiation and ferulic acid derivatives. Photochem. Photobiol. **91**, 1422-1428.

Shirai, A., Kawasaka, K., Tsuchiya, K., 2022a. Antimicrobial action of phenolic acids combined with violet 405-nm light for disinfecting pathogenic and spoilage fungi. J. Photochem. Photobiol. B: Biol. **229**, 112411.

Shirai, A., Kunimi, H., Tsuchiya, K., 2022b. Antifungal action of the combination of ferulic acid and ultraviolet-A irradiation against *Saccharomyces cerevisiae*. J. Appl. Microbiol. **132**, 2957-2967.

Shirai, A., Watanabe, T., Matsuki, H., 2017. Inactivation of foodborne pathogenic and spoilage micro-organisms using ultraviolet-A light in combination with ferulic acid. Lett. Appl. Microbiol. **64**, 96-102.

Shirai, A., Yasutomo, Y., 2019. Bactericidal action of ferulic acid with ultraviolet-A light irradiation. J. Photochem. Photobiol. B: Biol. **191**, 52-58.

Stepanik, T., Kost, D., Nowicki, T., Gaba, D., 2007. Effects of electron beam irradiation on deoxynivalenol levels in distillers dried grain and solubles and in production intermediates. Food Addit. Contam. **24**, 1001-1006.

Sugita-Konishi, Y., Park, B.J., Kobayashi-Hattori, K., Tanaka, T., Chonan, T., Yoshikawa, K., Kumagai, S., 2006. Effect of cooking process on the deoxynivalenol content and its subsequent cytotoxicity in wheat products. Biosci., Biotechnol., Biochem. **70**, 1764-1768.

Suzuki, T., 2018. Light-irradiation wavelength and intensity changes influence aflatoxin synthesis in fungi. Toxins **10**, 31.

Wang, M., Jiang, N., Wang, Y., Jiang, D., Feng, X., 2017a. Characterization of phenolic compounds from early and late ripening sweet cherries and their antioxidant and antifungal activities. J. Agric. Food Chem. **65**, 5413-5420.

Wang, Q., de Oliveira, E.F., Alborzi, S., Bastarrachea, L.J., Tikekar, R.V., 2017b. On mechanism behind UV-A light enhanced antibacterial activity of gallic acid and propyl gallate against

624 *Escherichia coli* O157:H7. Scientific Reports **7**, 8325.

625 Wu, S., Wang, F., Li, Q., Wang, J., Zhou, Y., Duan, N., Niazi, S., Wang, Z., 2020. Photocatalysis
626 and degradation products identification of deoxynivalenol in wheat using upconversion
627 nanoparticles@TiO_2 composite. Food Chem. **323**, 126823.

628 Young, J.C., Zhu, H., Zhou, T., 2006. Degradation of trichothecene mycotoxins by aqueous
629 ozone. Food Chem. Toxicol. **44**, 417-424.

630 Zhou, Y., Wu, S., Wang, F., Li, Q., He, C., Duan, N., Wang, Z., 2020. Assessing the toxicity in
631 vitro of degradation products from deoxynivalenol photocatalytic degradation by using
632 upconversion nanoparticles@TiO_2 composite. Chemosphere **238**, 124648.

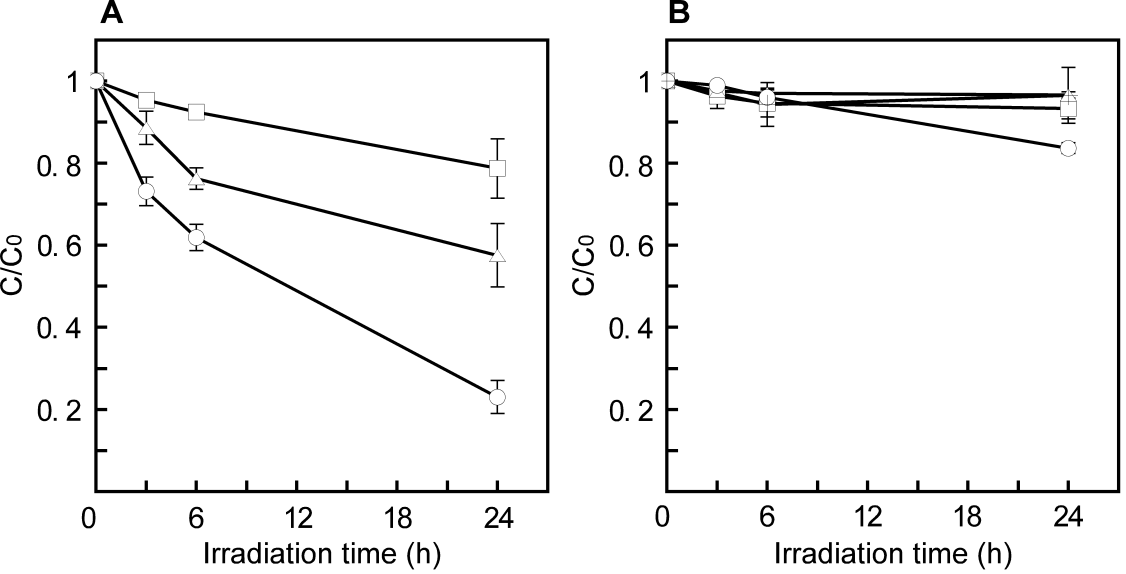

Fig. 1.

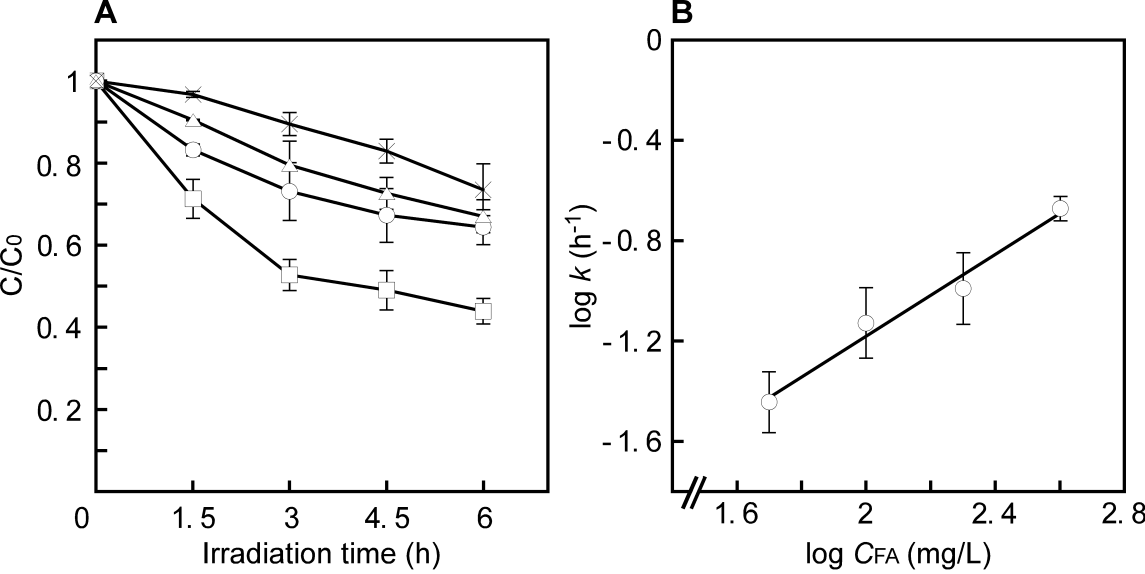

Fig. 2.

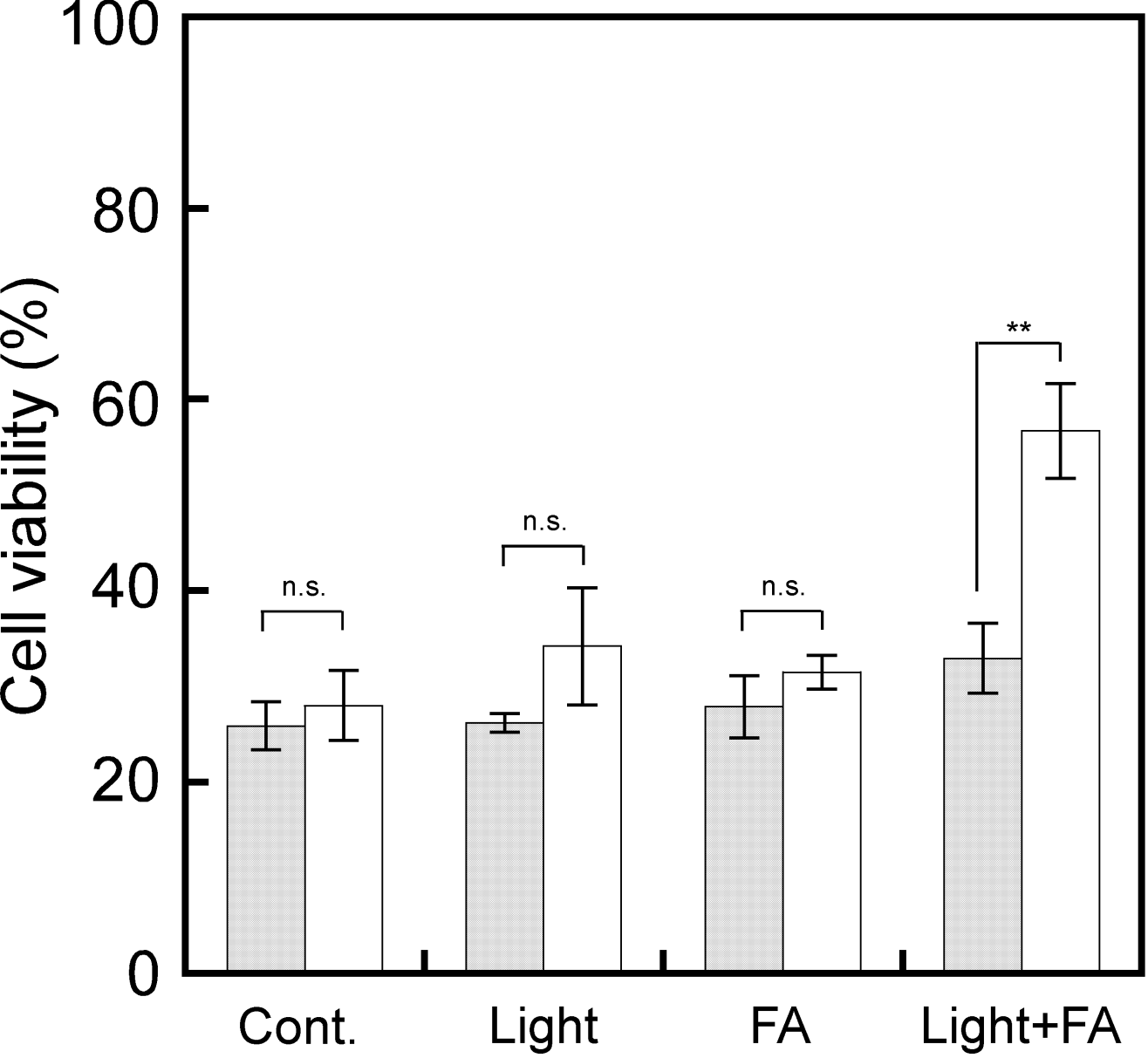

Fig. 3.

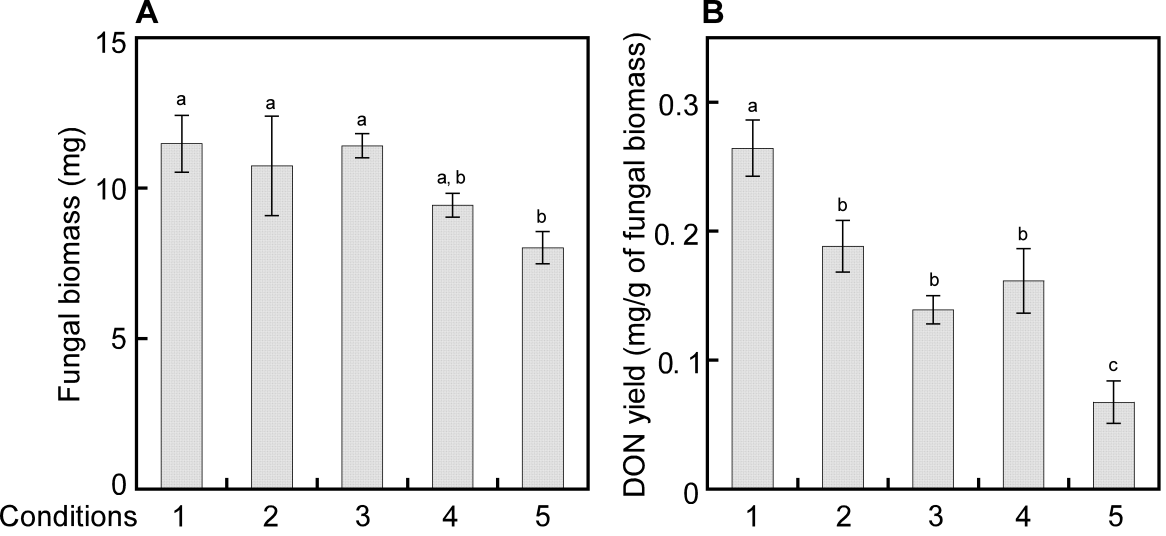
A
B
Fungal biomass (mg)
DON yield (mg/g of fungal biomass)
Conditions
15
10
5
0
0.3
0. 2
0. 1
0
a
a
a
a, b
b
a
b
b
b
c
1
2
3
4
5

Fig. 4.

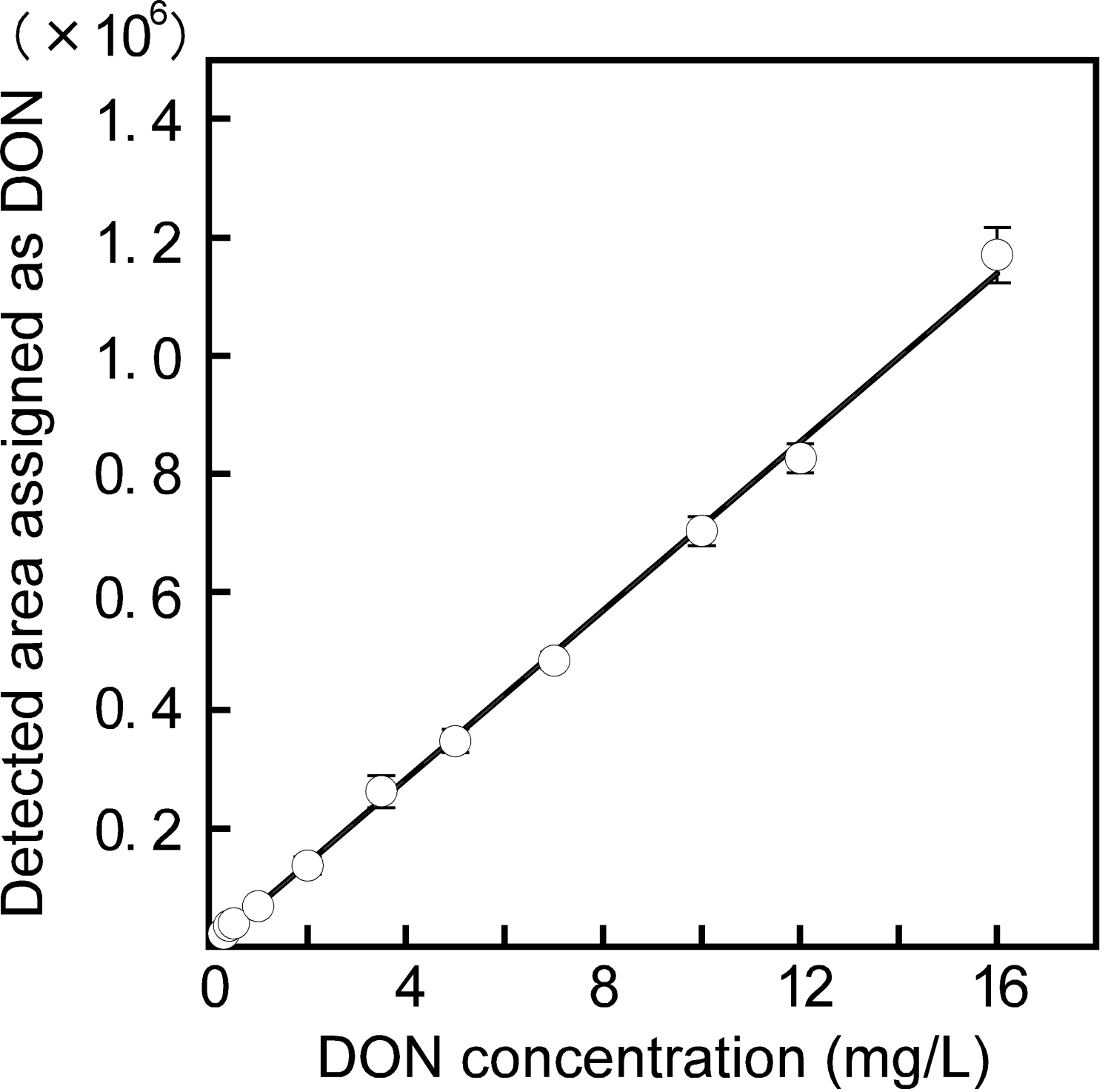
(× 10^6)
Detected area assigned as DON
1. 4
1. 2
1. 0
0. 8
0. 6
0. 4
0. 2
0
4
8
12
16
DON concentration (mg/L)

Fig. A.1.

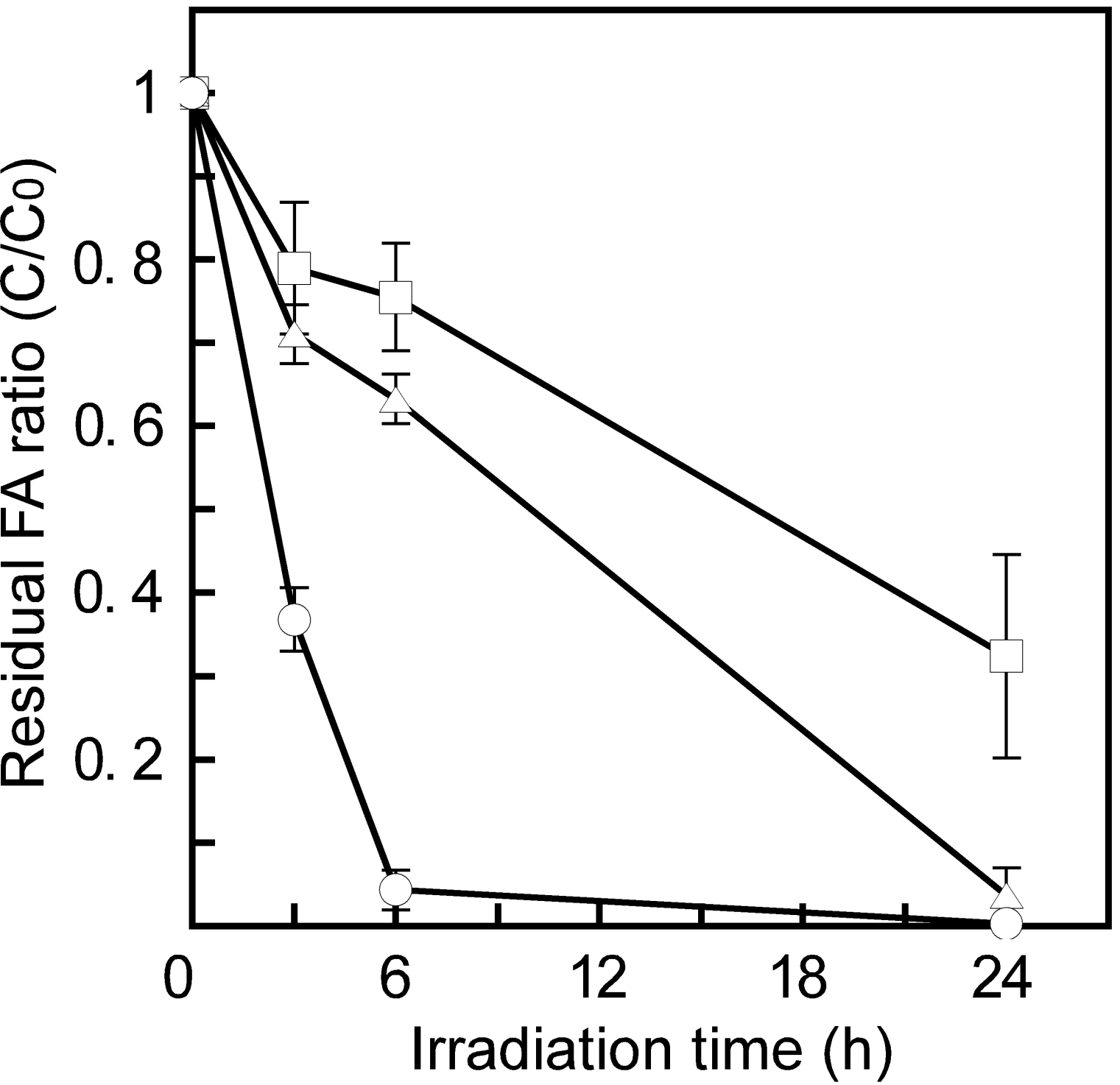
Residual FA ratio (C/C0)
1
0. 8
0. 6
0. 4
0. 2
0
6
12
18
24
Irradiation time (h)

Fig. B.1.

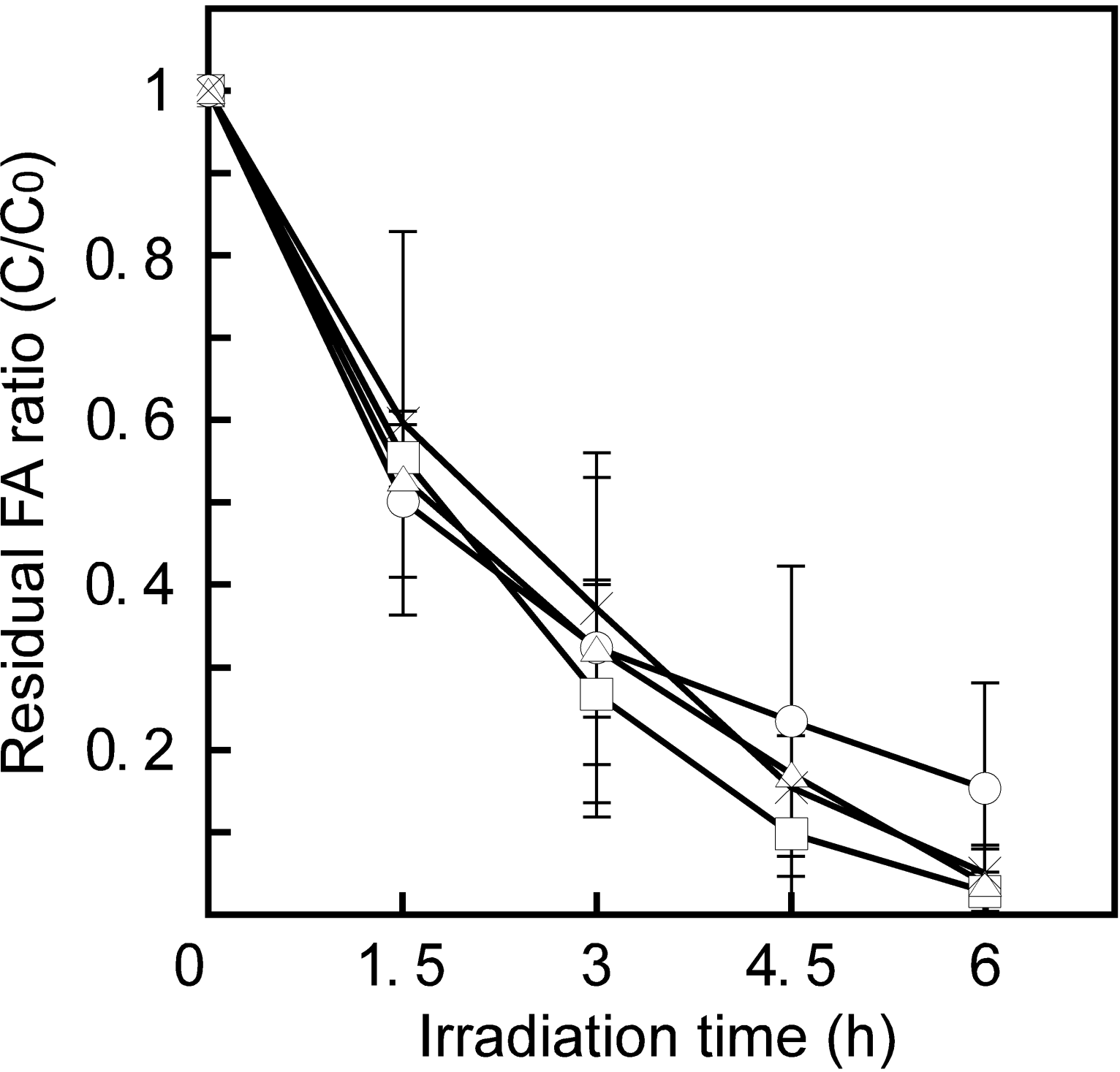
Residual FA ratio (C/C0)
1
0. 8
0. 6
0. 4
0. 2
0
1. 5
3
4. 5
6
Irradiation time (h)

Fig. C.1.

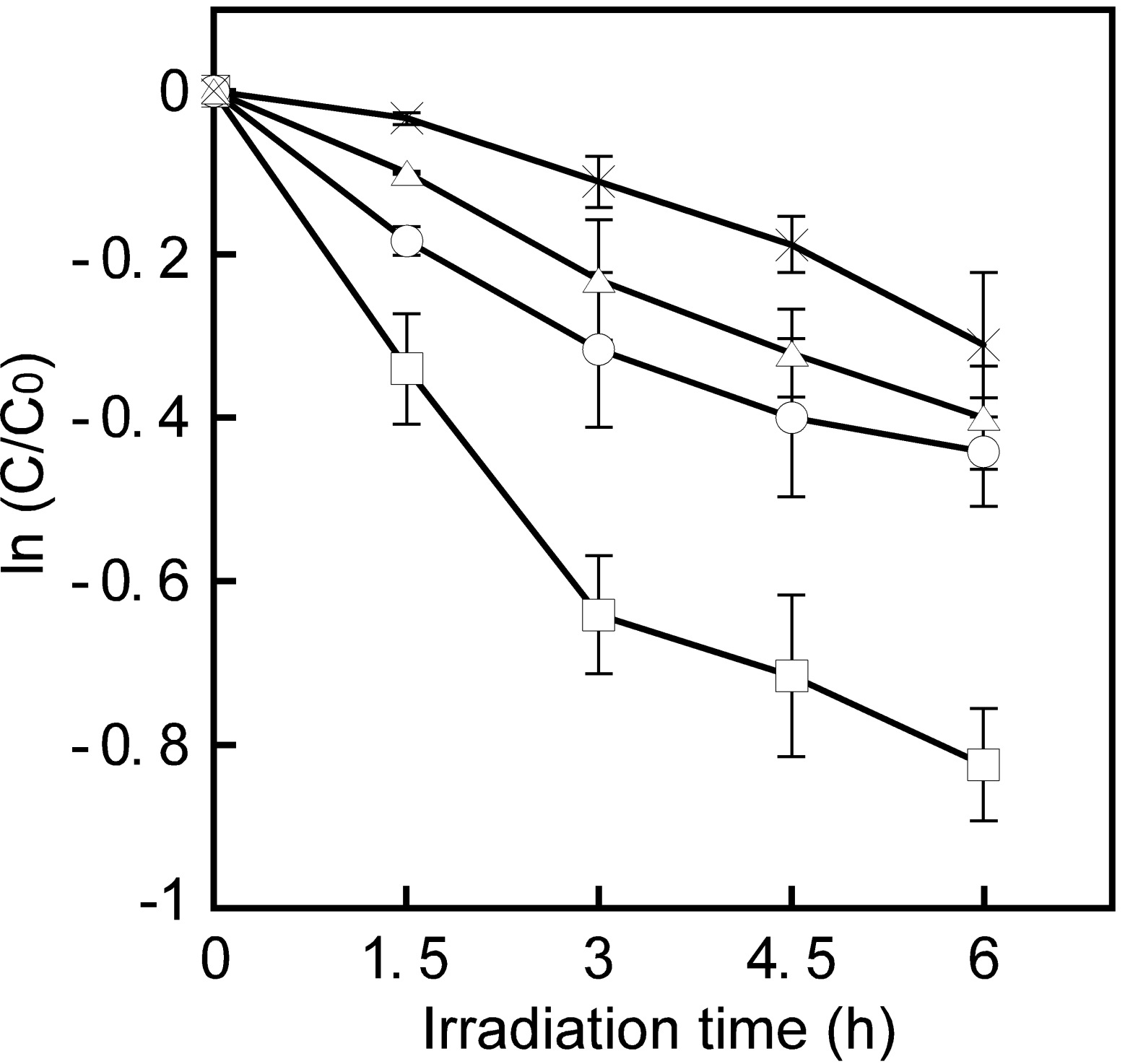

Fig. C.2.